

SURFACE WAVE CHARACTERISTICS AND 2D ELECTROMAGNETIC FIELD DISTRIBUTION IN ATMOSPHERIC PRESSURE PLASMA COLUMN

M. Pencheva, E. Benova

St. Kliment Ohridski University of Sofia, Sofia, Bulgaria

1. Introduction

There is a growing interest in the propagation of electromagnetic (EM) waves in atmospheric pressure plasmas (APP). It is due to the applications of this phenomenon in many fields, such as electron density diagnostic of APP [1,2] as well as in the industry [3]. Numerical simulations have already shown that the APP can absorb the EM wave and the attenuation of the EM wave passed through the plasma layer depends on the frequency of the EM wave and on the parameters of the plasmas such as the electron–neutral collision frequency [1–3]. Plasma sustained by surface wave is quite different set-up from a wave propagating through a plasma layer. Yet it can be used for studying the interaction between an EM field and plasma since this interaction is its essential feature.

In this study the effect of the collisions between electrons and neutrals on the characteristics of a surface wave (SW) maintaining plasma at atmospheric pressure is investigated. Two set-ups are considered, plasma–vacuum and plasma–dielectric–vacuum. The values ν of the electron–neutral collision frequencies used for studying the collisional damping effect are drawn from the collisional–radiative model for argon discharge [4] at atmospheric pressure which is applied for typical experimental conditions.

2. Theoretical description

We consider high frequency azimuthally symmetric SW propagating along plasma column with radius R that is placed in dielectric tube with radius R_d surrounding by air (vacuum). Maxwell equations are used for describing the behaviour of the wave in the three media [5]. All of them are considered as dielectrics with dielectric permittivity ϵ_p , ϵ_d and $\epsilon_v = 1$ for the plasma, dielectric and vacuum respectively, where:

$$\epsilon_p = 1 - \frac{\omega_p^2}{\omega(\omega + i\nu)} = 1 - \frac{\omega_p^2}{\omega^2} \left(1 + \frac{\nu^2}{\omega^2} \right)^{-1} + i \frac{\nu}{\omega} \frac{\omega_p^2}{\omega^2} \left(1 + \frac{\nu^2}{\omega^2} \right)^{-1} \quad (1)$$

with ω_p being the usual electron plasma angular frequency and ν – the electron–neutral collision frequency for momentum transfer.

In WKB approximation one seeks the solutions for the wave components in the form:

$$\begin{aligned} B_\phi(r, z) &= \text{Re} \left[G_\phi(r) B(z) \exp(-i\omega t + i \int_0^z dz' k(z')) \right] \\ E_{r,z}(r, z) &= \text{Re} \left[F_{r,z}(r) E(z) \exp(-i\omega t + i \int_0^z dz' k(z')) \right] \end{aligned} \quad (2)$$

In these expressions $k = k'R + ik''R$ is the dimensionless complex wave number, k' being the axial wave number, k'' the attenuation coefficient; $E(z) = B(z) \equiv E_{r,z}(r = R)$, and F_z, F_r, G_ϕ are the cylindrical functions, solutions of the dimensionless wave equations.

Applying the boundary conditions for continuity of the tangential components the analytical forms of the field components and the local (for fixed z) dispersion relation (LDR) are derived. Their explicit form can be found in Ref. [6]. LDR provides a dependence of the real and the imaginary part of the wave number on the plasma frequency (the so called phase and attenuation diagram) at fixed wave frequency.

3. Results and discussions

The calculations are done for tube dielectric permittivity $\epsilon_d = 4$ and dimensionless width $\gamma = R_d/R = 2.5$. The zero of the z axis is set at the end of the plasma column while the wave launcher is at position 0.35 m (the length of the discharge).

Figure 1 presents the spatial distribution of the components of the surface wave electromagnetic field within the plasma spatial domain. The plasma density is $n_e = 7 \times 10^{20} \text{ m}^{-3}$. It can be seen that from the launcher toward the end of the discharge the amplitude F_z of the axial component at the discharge axis increases which means the wave gradually penetrates into the plasma keeping the amplitude of the component at the surface of the column almost constant. The radial component F_r of the EM field grows more than three times as the plasma density along the discharge decreases. But it is still considerably smaller than the axial one.

In Figure 2 the wave components in the discharge, the dielectric tube and the surrounding vacuum are shown and one can get the picture of the field distribution outside the plasma. All the components decrease with the distance from the launcher as it is expected. The descending trend of the axial component is close to linear while for the radial component it is much stronger especially at the end of the column. In radial direction the continual axial component gradually grows in the plasma–dielectric domain having its maximum at the

dielectric–vacuum interface and then diminishes in the vacuum. The radial component is discontinuous along the radius being maximal in the vacuum and more precise at the dielectric–vacuum surface.

The effect of the electron–neutral collision frequency ν on the wave field is depicted in figure 3. Two configurations are examined – plasma–vacuum and plasma–dielectric–vacuum. The increase of the collisions between electrons and atoms results in increase of the damping of all wave

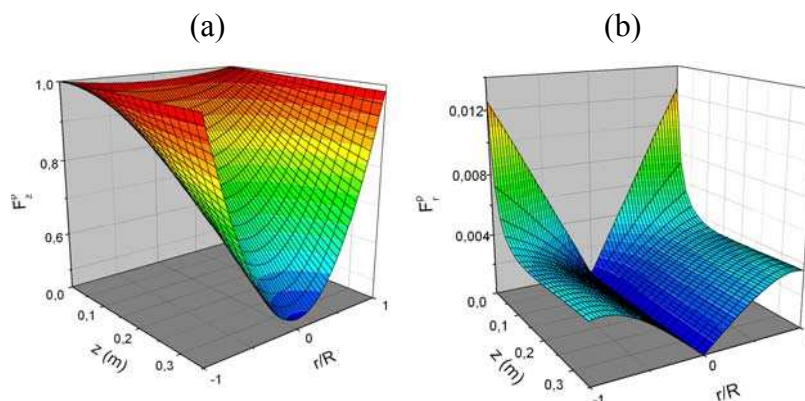


Figure 1. Spatial (radial and axial) distribution of the axial (a) and radial (b) surface wave components within the plasma.

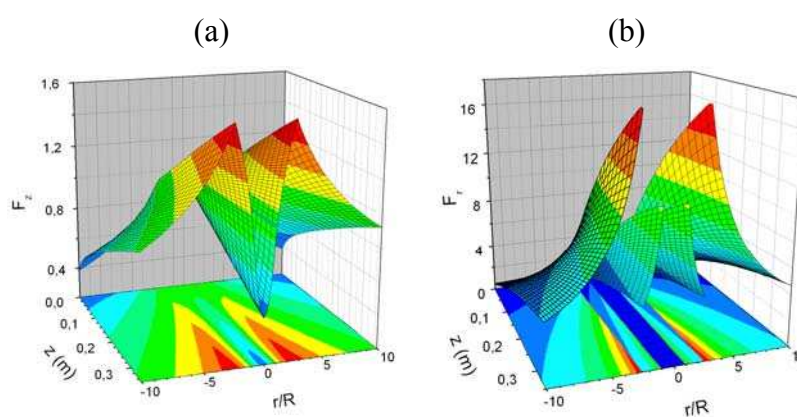


Figure 2. Spatial distribution of the axial (a) and radial (b) wave components for configuration plasma ($|r|/R < 1$), dielectric ($1 < |r|/R < 2.5$) and vacuum ($|r|/R > 2.5$)

components outside the plasma. But inside the plasma domain both the axial and the radial electric field component grow. This results in almost constant axial field inside the plasma for the highest ν (Figure 3a) while the radial component F_r rises at the plasma surface but then rapidly decreases in the plasma bulk (Figure 3b). For smaller collision frequencies the F_z component has its maximum at the dielectric–vacuum interface but for higher ν it moves at the plasma–dielectric surface. The radial component of the wave is maximal in the vacuum; more than two times lower in the dielectric and almost negligible ($F_r < 0.01$) within the plasma for any ν . Similar dependences are observed at low pressure (see Ref. [7]).

The phase and attenuation diagrams – the dependences of the propagation $k'R$ and attenuation $k''R$ coefficients on the plasma density are plotted in Figure 4 for the two considered configurations and for different collision frequencies ν . The increase of the collisions eliminates the effect of the dielectric. One can see that at the lowest ν the maximum values (marked on the curves with open circles) of both the dimensionless wave number,

presented by its real k' and imaginary k'' part, and the plasma density n (entering in the plasma frequency $\omega_p = (4\pi e^2 n / m)^{1/2}$) in the case of plasma–vacuum are much higher than in plasma–dielectric–vacuum structure. While at higher collision frequencies the difference is very small.

4. Conclusions

The spatial distributions of the components of EM field sustaining a SW discharge are obtained and the influence of the electron–neutral collision

frequency on the wave characteristics is studied. It is found out that the increase of ν facilitate the penetration of the wave into the plasma and diminishes the influence of the dielectric tube on the field properties.

5. Acknowledgements

This work was supported by the Fund for Scientific Research of the University of Sofia under Grant 107/2009.

References

[1] Zhang S and Hu X W 2005 *Chin. Phys. Lett.* **22** 168
 [2] Zhang S, Hu X W, Jiang Z H, Liu M H and He Y 2006 *Phys. Plasmas* **13** 013502
 [3] Guo B and Wang X G 2005 *Phys. Plasmas*. **12** 084506
 [4] Pencheva M, Petrov G, Petrova Ts, and Benova E 2004 *Vacuum* **76** 409 – 412
 [5] Pencheva M, Benova E, Zhelyazkov I 2007 *Journal of Physics: Conference Series* **63** 012023
 [6] Zhelyazkov I, Atanassov V 1995 *Physics Reports* **255** 79 – 201
 [7] Zethoff M, Kortshagen U 1992 *J. Phys. D: Appl. Phys.* **25** 1575 – 1582

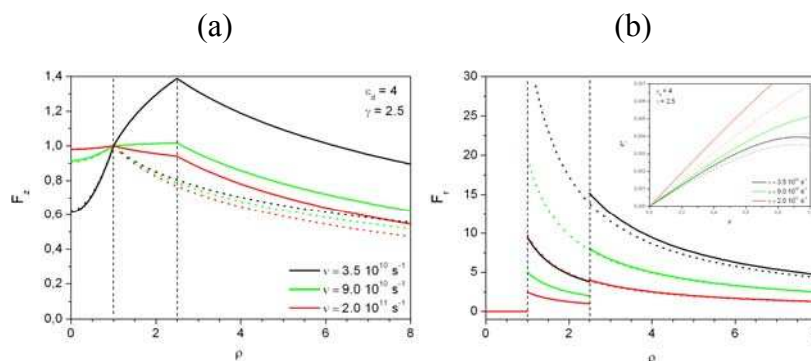


Figure 3. Dependence of the radial distribution of the axial (a) and radial (b) surface wave components on the collision frequency for configuration plasma–dielectric–vacuum – the solid lines and plasma–vacuum – the dotted lines.

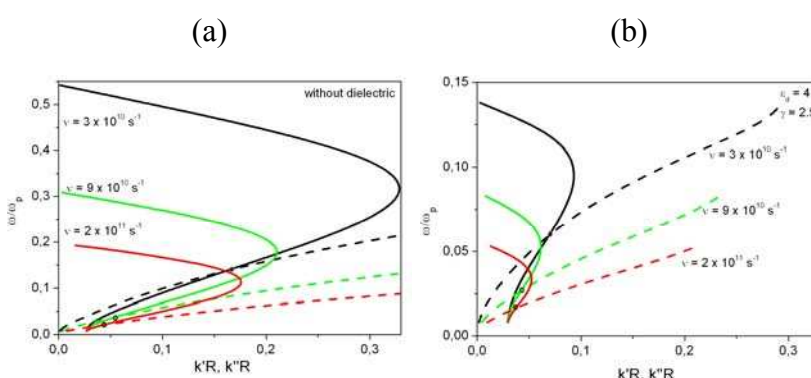


Figure 4. Dependence of the dimensionless propagation (solid lines) and attenuation (dashed lines) wave coefficients, e.g. the phase and attenuation diagrams on the collision frequency for configuration (a) plasma–vacuum and (b) plasma–dielectric–vacuum.